Use of $^{13}C-^{1}H$ NMR Coupling Constants To Assess the Binding of Imidazole Ring Ligands to Metals

Scott J. Moore,[†] Rene J. Lachicotte,[‡] Sharon T. Sullivan,[†] and Luigi G. Marzilli*,[†]

Department of Chemistry, Emory University, Atlanta, Georgia 30322, and Department of Chemistry, University of Rochester, Rochester, New York 14627

Received May 7, 1998

In this report we initiate analysis of imidazole rings bound to metals using one−bond ^{1}H-^{13}C couplings. Shift trends in the metal binding of N-donor heterocyclic ligands have been difficult to interpret since signals of close-in nuclei, particularly the carbon in the CN_2 grouping of imidazole rings, often have erratic or small shift changes. We exploit the well-studied trans influence of a series of unidentate axial R and X ligands in cobaloxime complexes ($LCo(DH)_2$(R or X)) since shifts of carbons remote from Co have interpretable trends that correlate with Co−N bond lengths. We compare information obtained from $^{1}J_{CH}$ values for two series, one with L = a small ligand, *N*-methylimidazole (*N*-MeImd), and one with L = a large ligand, 1,5,6-trimethylbenzimidazole (Me_3Bzm). For comparison to our spectroscopic measurements, we have determined X-ray crystal structures for *N*-MeImdCo-$(DH)_2$(R or X) (where DH = monoanion of dimethylglyoxime, R or X = CH_2CH_3 (**1**), CH_3 (**2**), CH_2CN (**3**), and Cl (**4**)) doubling the number of structures reported for cobaloximes containing *N*-MeImd. The observation of the B-type orientation of the planar *N*-MeImd axial ligand in structures 1 and 2 almost certainly results from the small size of *N*-MeImd. This B-orientation is rare for cobaloximes, which normally have an axial ligand in the A-orientation. The *t* scores obtained from the principal component analysis of cobaloxime data [Randaccio, L.; Geremia, S.; Zangrando, E.; Ebert, C. *Inorg. Chem.* **1994**, *33*, 4641] were applied for the first time in the analysis of intraligand coupling constants. The use of these parameters allowed us to identify steric effects on the ^{13}C shifts and $^{1}J_{CH}$ values for the bulky, lopsided Me_3Bzm axial ligand in the Me_3BzmCo(DH)(R or X) series; similar steric effects on spectra were not observed for *N*-MeImdCo(DH)(R or X). The intraligand $^{1}J_{CH}$ values for the close-in N_2CH carbon of Me_3Bzm and *N*-MeImd were found to reflect the ligand-to-metal binding even better than the more commonly used ^{13}C shifts of carbons remote from the metal. Thus, the use of $^{1}J_{CH}$ values holds considerable promise in metallobiochemistry.

Introduction

Imidazole rings (nucleic acids, proteins, antibiotics, and cofactors) are prevalent in biological systems serving roles in acid/base chemistry, catalysis, H-bonding, and in metal complexation. Changes in the ^{13}C NMR shifts of these heterocyclic compounds bound to metals either yield little useful information or require complicated interpretations (e.g., histidine in the Zn·bleomycin complex,[1] C8 of purines bound to cis-type Pt anticancer drugs,[2] and the axial dimethylbenzimidazole of cobalamins[3]). We have previously reported a reliable means of obtaining high-resolution coupling constants for the CH group linking the ring nitrogens and the potential usefulness of such data in assessing the nature of the imidazole ring.[4]

In addition to through-bond effects, ^{13}C chemical shifts in complexes relevant to metallobiochemistry are typically influenced by through-space effects. For these reasons, cobalamins and their related model complexes are one system in which ^{13}C shifts have been characteristically difficult to interpret.[5,6] Early studies of the ^{13}C shifts in cobaloxime B_{12} models indicated an anisotropic influence of the metal on ligand atoms near the coordination site.[7] To minimize such through-space effects, the ^{13}C shifts of the remote γ carbon in pyridine (py) cobaloximes ($LCo(DH)_2$(R or X), where $(DH)_2$ = monoanion of dimethylglyoxime, L = py, Chart 1) were used to assess the trans influence. A scale was developed and each R or X ligand was characterized by a numerical value called the electronic parameter, EP.[8] Attempts to account for through-space effects on shifts while examining C atoms closer to the metal binding site with cobalamins and later with cobaloximes have met with limited success.[5,6] These methods describe the variation in ^{13}C chemical shifts as a combination of an electronic inductive parameter and a geometric/anisotropic parameter. This dual-parameter approach was applied to the interpretation of ^{13}C shifts of cobaloximes containing 1,5,6-trimethylbenzimidazole (Me_3Bzm). The results indicated that equatorial ligand anisotropy has a more significant effect than Co anisotropy on ^{13}C shifts in cobalamins for atoms near the axial coordination site.[5] In addition to these through-space anisotropic effects, the methods depend on the shift difference between the free and complexed ligand; however, there is no easy way to allow for the effect on shifts of differences in solvation of the ligand when

[†] Emory University.
[‡] University of Rochester.

(1) Calafat, A. M.; Won, H.; Marzilli, L. G. *J. Am. Chem. Soc.* **1997**, *119*, 3656.
(2) Mukundan, S., Jr.; Xu, Y.; Zon, G.; Marzilli, L. G. *J. Am. Chem. Soc.* **1991**, *113*, 3021.
(3) Calafat, A. M.; Marzilli, L. G. *J. Am. Chem. Soc.* **1993**, *115*, 9182.
(4) Moore, S. J.; Iwamoto, M.; Marzilli, L. G. *Inorg. Chem.* **1998**, *37*, 1169.
(5) Charland, J.-P.; Zangrando, E.; Bresciani-Pahor, N.; Randaccio, L.; Marzilli, L. G. *Inorg. Chem.* **1993**, *32*, 4256.
(6) Brown, K. L.; Hakimi, J. M. *J. Am. Chem. Soc.* **1986**, *108*, 496.
(7) Stewart, R. C.; Marzilli, L. G. *Inorg. Chem.* **1977**, *16*, 424.
(8) Zangrando, E.; Bresciani-Pahor, N.; Randaccio, L.; Charland, J.-P.; Marzilli, L. G. *Organometallics* **1986**, *5*, 1938.

10.1021/ic980519k CCC: $18.00
Published on Web 01/06/1999

Chart 1

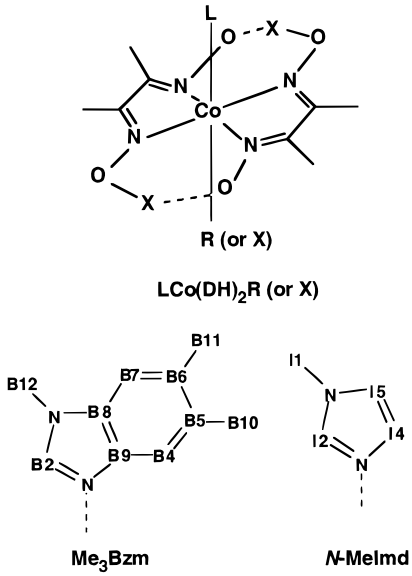

free and when bound. Furthermore, the methods to assess anisotropic effects on shifts require structural data for the determination of the geometric/anisotropic parameter. This reliance on X-ray crystallographic data limited the usefulness of the dual parameter approach to cobalamins since few structures were available.[6]

Unlike ^{13}C chemical shifts, one-bond proton−carbon coupling constants ($^1J_{CH}$) reflect through-bond influences in relative isolation from through-space effects.[4] The observed "pure" through-bond inductive effect arises because of the dominance of the Fermi contact term in spin−spin coupling of directly bound nuclei.[9] Hence, only the contribution of valence atomic s orbitals to molecular orbitals involved predominates in the description of $^1J_{CH}$ values.[10,11] Therefore, $^1J_{CH}$ values for the L ligand can be used to probe changes in s orbital contribution in the CH bond in response to changes in the electron-donating ability of the trans ligand.[12] In fact, $^1J_{CH}$ values have been used to quantify the percentage of s character in the C atom hybrid orbital of the CH bond.[10,11] In a study of a limited series of cobaloximes, we found good correlations between $^1J_{CH}$ values of coordinated Me_3Bzm and measures of the electron-donating ability of R.[4]

In this report, extending our initial assessment of the dependence of the intraligand CH coupling constants on variations in the trans influence of the trans ligand, we employ the cobaloxime B_{12} model complexes and investigate both Me_3Bzm or *N*-methylimidazole (*N*-MeImd, Chart 1) complexes. NMR data for these complexes have been analyzed in terms of measures of the trans influence (e.g., $Co-N_L$ bond distances and EP). In addition to these traditional parameters, we employed for the first time the results of Randaccio and coworkers' rigorous statistical treatment of published alkylcobaloxime data.[13]

Experimental Section

Materials and Preparations. Me_3Bzm was prepared as reported.[14] All other reagents were obtained from Aldrich and used without further purification. $LCo(DH)_2R$ [L = Me_3Bzm, R = CH_2Br, $CH(CN)CH_2CN$; and L = *N*-MeImd, R = CH_2CH_3 (**1**), CH_3 (**2**), CH_2Br, $CH(CN)CH_2CN$] were prepared by the standard method,[15,16] reduction of $LCo(DH)_2Cl$ with $NaBH_4$ in the presence of the appropriate alkylating agent. $H_2OCo(DH)_2R$ complexes were prepared by treatment of $pyCo(DH)_2R$ with a strongly acidic resin as described previously.[17] $LCo(DH)_2R$ (L = Me_3Bzm, R = CH_2CF_3, $CH(CH_3)_2$, adamantyl (adam); and L = *N*-MeImd, R = CH_2CF_3, $CH(CH_3)_2$, CH_2CN (**3**), adam) complexes were prepared from $H_2OCo(DH)_2R$ as previously described.[5,17,18] $Me_3BzmCo(DH)_2N_3$ was prepared as previously reported.[19]

The preparation of $LCo(DH)_2Cl$ (L = Me_3Bzm, *N*-MeImd (**4**)) was analogous to that described for (4-*t*-Bupy)$Co(DH)_2Cl$.[20] *N*-MeImd$Co(DH)_2CH_2OCH_3$ was prepared according to the procedure reported for $Me_3BzmCo(DH)_2CH_2OCH_3$.[21] $Me_3BzmCo(DH)_2CH_2NO_2$ was prepared from $Me_3BzmCo(DH)_2Cl$ using a method analogous to that for $pyCo(DH)_2CH_2NO_2$.[22]

All complexes were obtained in 50−90% yield. C, H, and N analyses (Atlantic Microlabs, Inc., Norcross, GA) for new complexes were satisfactory (Supporting Information).

X-ray Structural Determinations. All X-ray structures except that of *N*-MeImd$Co(DH)_2Cl$ (**4**) were obtained on a Siemens CCD SMART Area Detector System equipped with a normal focus molybdenum-target X-ray tube operated at 2.0 kW (50 kV, 40 mA). Crystals of *N*-MeImd$Co(DH)_2CH_2CH_3$ (**1**), *N*-MeImd$Co(DH)_2CH_3$ (**2**), and *N*-MeImd$Co(DH)_2CH_2CN$ (**3**) were obtained by slow evaporation from concentrated Me_2CO/EtOAc/Bz (∼ 60:20:20) solutions of the respective complexes. Each crystal was mounted under Paratone-8277 on a glass fiber, and immediately placed in a cold nitrogen stream at either −80 °C (**1**) or −90 °C (**2**, **3**) on the X-ray diffractometer. The 1321 frames of data (1.3 hemispheres) were collected using a narrow frame method with scan widths of 0.3° in ω and exposure times of 30 s/frame using a detector-to-crystal distance of 5.09 cm. The total data collection time was ∼12 h.

Frames were integrated to 0.90 Å for **1** and **2** and to 0.75 Å for **3** with the Siemens SAINT program. Laue symmetry revealed an orthorhombic crystal system for both **1** and **3** and a monoclinic crystal system for **2**. Final unit cell parameters were determined from the least-squares refinement of three-dimensional centroids of 6965, 4282, and 8192 reflections for **1**, **2**, and **3**, respectively. Data for all structures were corrected for absorption with the SADABS[23] program.

Space groups were assigned on the basis of systematic absences and are reported in Table 1. Each structure was solved by using direct methods and refined employing full-matrix least-squares on F^2 (Siemens, SHELXTL[24]). For each structure, all of the non-hydrogen atoms were refined with anisotropic thermal parameters. The C(9) methyl protons for 1, and the bridging oxime protons (H1 and H2) for all the structures, were located and their positions and isotropic thermal parameters refined. All other hydrogen atoms were included in idealized positions giving data/parameter ratios >10:1. For each structure, the final difference map showed no residual electron density greater than 0.69 $e^-/Å^3$. The structures refined to goodness-of-fit (GOF)[25] values of ∼1.0. Final residuals are listed in Table 1.

(9) Harris, R. K. *Nuclear Magnetic Resonance Spectroscopy: A Physiochemical View*; John Wiley & Sons: New York, 1986; p 260.
(10) Drago, R. S. *Physical Methods for Chemists*, 2nd ed.; Saunders College Publishing: New York, 1992; p 251.
(11) (a) Muller, N. *J. Chem. Phys.* **1962**, *36*, 359. (b) Goldstein, J. H.; Reddy, G. S. *J. Chem. Phys.* **1962**, *36*, 2644.
(12) Moore, S. J.; Marzilli, L. G. *Inorg. Chem.* **1998**, *37*, 5329.
(13) Randaccio, L.; Geremia, S.; Zangrando, E.; Ebert, C. *Inorg. Chem.* **1994**, *33*, 4641.
(14) Simonov, A. M.; Pozharskii, A. E.; Marianovskii, V. M. *Indian J. Chem.* **1967**, *5*, 81.
(15) Hill, H. A. O.; Morallee, K. G. *J. Chem. Soc. A* **1969**, 554.
(16) Stewart, R. C.; Marzilli, L. G. *J. Am. Chem. Soc.* **1978**, *100*, 817.
(17) Toscano, P. J.; Chiang, C. C.; Kistenmacher, T. J.; Marzilli, L. G. *Inorg. Chem.* **1981**, *20*, 1513.
(18) Marzilli, L. G.; Summers, M. F.; Zangrando, E.; Bresciani-Pahor, N.; Randaccio, L. *J. Am. Chem. Soc.* **1986**, *108*, 4830.
(19) Polson, S. M.; Cini, R.; Pifferi, C.; Marzilli, L. G. *Inorg. Chem.* **1997**, *36*, 314.
(20) Trogler, W. C.; Stewart, R. C.; Epps, L. A.; Marzilli, L. G. *Inorg. Chem.* **1974**, *13*, 1564.
(21) Cini, R.; Moore, S. J.; Marzilli, L. G. *Inorg. Chem.* **1998**, *37*, 6890.
(22) Randaccio, L.; Bresciani-Pahor, N.; Toscano, P. J.; Marzilli, L. G. *Inorg. Chem.* **1981**, *20*, 2722.
(23) The SADABS program is based on the method of Blessing; see: Blessing, R. H. *Acta Crystallogr., Sect A* **1995**, *51*, 33.
(24) *SHELXTL: Structure Analysis Program*, version 5.04; Siemens Industrial Automation Inc.: Madison, WI, 1995.

Table 1. Summary of Crystallographic Data for Complexes **1**−**4**

crystal params	**1**	**2**	**3**	**4**
empirical formula	$C_{14}H_{25}CoN_6O_4$	$C_{13}H_{23}CoN_6O_4$	$C_{14}H_{22}CoN_7O_4$	$C_{12}H_{20}ClCoN_6O_4$
fw	400.33	386.30	411.32	406.72
cryst syst	orthorhombic	monoclinic	orthorhombic	triclinic
space group (no.)	*Pbca* (61)	$P2_1/n$ (14)	$P2_12_12_1$ (19)	$P\bar{1}$ (2)
Z	8	4	4	2
a, Å	10.9234(1)	9.1481(1)	9.8297(1)	8.978(2)
b, Å	15.8804(2)	11.4177(2)	11.1519(1)	9.014(2)
c, Å	20.7466(2)	16.2156(1)	16.1352(2)	11.480(3)
α, deg				86.059(18)
β, deg		96.78(0)		84.022(17)
γ, deg				68.483(12)
volume, Å^3	3598.87(7)	1681.88(4)	1768.74(3)	859.1(3)
ρ_{calc}, mg mm^{-3}	1.478	1.526	1.545	1.572
cryst dimens, mm^3	0.08 × 0.24 × 0.30	0.12 × 0.20 × 0.36	0.28 × 0.30 × 0.38	0.40 × 0.40 × 0.16
temp, °C	−80	−90	−90	−100
	Measurement of Intensity Data and Refinement Parameters			
radiation (*λ*, Å)	Mo Kα (0.710 73)	Mo Kα (0.710 73)	Mo Kα (0.710 73)	Mo Kα (0.710 73)
2*θ* range, deg	2−46	4−46.9	4.5−56.8	3.56−44.98
data collcd	$-7 \le h \le 12$, $-17 \le k \le 17$, $-21 \le l \le 23$	$-10 \le h \le 10$, $-12 \le k \le 11$, $-17 \le l \le 18$	$-12 \le h \le 13$, $-14 \le k \le 7$, $-21 \le l \le 21$	$-1 \le k \le 9$, $-9 \le k \le 9$, $-12 \le l \le 12$
no. of data collcd	13729	7153	11348	2760
no. of unique data	2594	2434	4268	2241
R_{int}, R_{sigma} (%)[a]	3.85, 2.78	3.75, 4.29	2.39, 3.21	1.76, 3.19
no. of obs. data ($I > 2\sigma(I)$)	2285	1994	3947	2019
no. of params varied	234	237	243	218
μ, mm^{-1}	0.986	1.052	1.007	1.184
absorption correction	empirical (SADABS)	empirical (SADABS)	empirical (SADABS)	empirical (*ψ* scans)
range of transm factors	0.65−0.90	0.65−0.93	0.65−0.89	0.425−0.820
R1(F_o), wR2(F_o^2)				
obs. (%)[b]	4.75, 10.24	4.14, 10.47	2.72, 7.10	4.10, 13.18
all (%)	6.01, 10.75	5.28, 10.94	3.04, 7.24	4.54, 13.83

[a] $R_{int} = \sum|F_o^2 - F_o^2(\text{mean})|/\sum[F_o^2]$; $R_{sigma} = \sum[\sigma(F_o^2)]/\sum[F_o^2]$. [b] $R1 = (\sum||F_o| - |F_c||)/\sum|F_o|$; $wR2 = [\sum[w(F_o^2 - F_c^2)^2]/\sum[w(F_o^2)^2]]^{1/2}$, where $w = 1/[\sigma^2(F_o^2) + (aP)^2 + bP]$ and $P = [\text{Max}(0, F_o^2) + 2F_c^2]/3$.

An amber-colored thin plate obtained on cooling a CH_2Cl_2/CH_3OH solution of **4** was mounted under oil on a copper pin. The crystal was placed in a cold N_2 stream at −100 °C, and intensity data were collected using a Siemens P4 diffractometer using graphite-monochromatized Mo Kα radiation. The unit cell was determined from least-squares refinement of 31 reflections ($4.8° \le 2\theta \le 24.9°$) Three check reflections were measured every 97 reflections with no significant deviation in intensity. Data were corrected for Lorentz and polarization effects. Empirical absorption corrections were performed from *ψ* scans. The structure was solved by Patterson methods and refined by full-matrix least-squares procedures.[24] All non-hydrogen atoms were refined using anisotropic thermal parameters. Hydrogen atoms were affixed to appropriate atoms with a data/parameter ratio of 10.3:1. The structure was refined to a GOF value of ∼1.2. Final residuals are listed in Table 1.

NMR Spectroscopy. All spectra were collected on 50−100 mM samples in $CDCl_3$ at 25 °C on a GE GN-600 Omega spectrometer (except as noted) and referenced to TMS. When available, reported ^{13}C NMR shifts for $Me_3BzmCo(DH)_2L$ in $CDCl_3$ were used.[4,5] ^{13}C NMR spectra of *N*-MeImd, *N*-MeImdCo(DH)$_2$R (or Cl), and additional $Me_3BzmCo(DH)_2R$ complexes were obtained on a GE QE-300 spectrometer. High-resolution $^1J_{CH}$ (±0.2 Hz) were obtained via the recently reported JHMQC (*J*-coupled heteronuclear multiple quantum coherence) method.[4] HMQC (heteronuclear multiple quantum coherence) and HMBC (heteronuclear multiple bond correlation) spectra were acquired for several Me_3Bzm complexes to assign closely spaced signals in the JHMQC spectra.

Statistical Analyses. The data were analyzed using the program JMPIN (version 3.1.5, SAS Institute, Inc.) to generate least-squares regression equations of the general form $Y = a_1X_1 + c$ (where Y = experimentally measured dependent variable; c = constant; a = coefficient; X_1 = independent variable). Coefficients of determination (r^2) were adjusted[26] to reflect the number of data points (n) according to the equation $r_a^2 = 1 - (1 - r^2)(n - 1)/(n - 2)$. Since negative values are meaningless for r^2, a value of zero is given when r_a^2 is <0. As n increases, r_a^2 approaches r^2, which represents the fraction of the total variance of the data set that is represented by the least-squares fit of the data. The analyses also included ANOVA (analysis of variance) tables including F tests indicating the significance level (p) of each parameter used.[26] Values of $p \le 0.0010$ were interpreted as significant, while values of $p < 0.0001$ were interpreted as highly significant. The $p \le 0.0010$ significance level corresponds to $r_a^2 \approx 0.80$ for $n = 13$, $r_a^2 \approx 0.90$ for $n = 9$, and $r_a^2 \approx 0.99$ for $n = 5$.

Results

Structures. The ORTEP representations of complexes **1**−**4** in Figures 1−4 show all non-hydrogen atoms and the atom numbering scheme. Selected bond distances and angles for these and related structures are presented in Table 2. Although a structure determined in the $P2_1/c$ space group [cell dimensions: $a = 9.25(1)$ Å; $b = 11.77(1)$ Å; $c = 19.80(1)$ Å; $\beta = 124.4(1)°$] has been reported (R = CH_3),[27] the crystal of **2** used here was determined in $P2_1/n$ and was obtained from a pure sample as confirmed by elemental analysis and ^{1}H NMR spectroscopy. Comparison of the two structures of **2** showed only small differences (Supporting Information). The cobalt atom had a distorted octahedral geometry with a displacement (d) from the least-squares plane of the four equatorial N atoms 0.025, 0.050, and 0.018 Å toward the *N*-MeImd for R =

(25) GOF = $[\sum[w(F_o^2 - F_c^2)^2]/(n - p)]^{1/2}$, where n and p denote the number of data and parameters.

(26) Daniel, W. W. *Biostatistics: A Foundation for Analysis in the Health Sciences*, 5th ed.; John Wiley & Sons: New York, 1991; p 740.

(27) Bigotto, A.; Zangrando, E.; Randaccio, L. *J. Chem. Soc., Dalton Trans.* **1976**, 96.

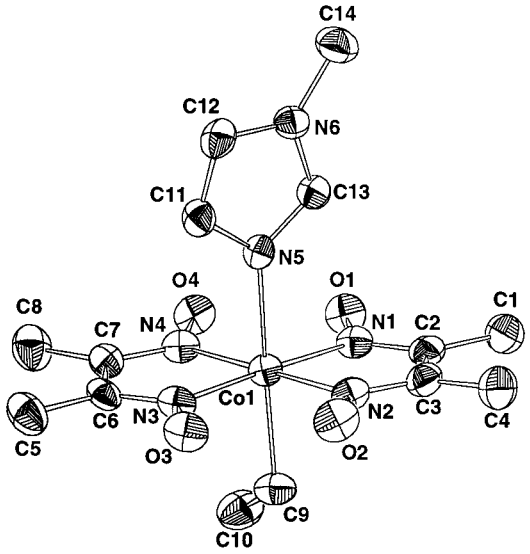

Figure 1. ORTEP drawing of *N*-MeImdCo(DH)$_2$CH$_2$CH$_3$ (**1**). Ellipsoids are shown at the 50% level. H atoms are omitted for clarity.

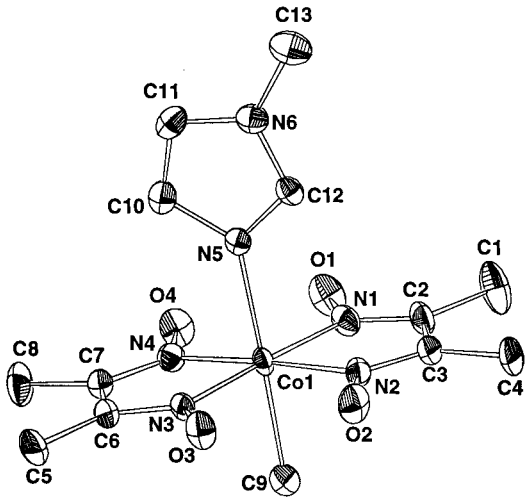

Figure 2. ORTEP drawing of *N*-MeImdCo(DH)$_2$CH$_3$ (**2**). Ellipsoids are shown at the 50% level. H atoms are omitted for clarity.

CH$_2$CH$_3$, CH$_3$, and Cl, respectively, and 0.018 Å toward the alkyl in R = CH$_2$CN. The two chemically equivalent DH moieties were nearly coplanar with dihedral angles for their mean planes (α) as reported in Table 2. For convenience during the discussion of both general structural features and NMR results, we have adopted the ligand numbering scheme (Chart 1) normally used for Me$_3$Bzm, B(#) and BH(#) for C and H atoms, respectively, and a similar scheme for *N*-MeImd, I(#) and IH(#) for C and H atoms, respectively.

(a) Orientation of the *N*-MeImd Plane. In all three structures, the *N*-MeImd ligand is nearly planar. The angle ϕ is defined as torsion angle I2−N$_L$−Co−N*, where N* is the midpoint between the N's of bridging O's on the side nearest I2. This angle has a value of 0° when I2 and N* are eclipsed. When viewed from the L side of the complex, negative ϕ values indicate a clockwise rotation around the Co−N$_L$ bond. This angle, reported for **1**−**4** in Table 2, allows for the classification of the ligand orientation as either A-type (∼0°) or B-type (∼90°, Chart 2). Cobaloximes such as those containing Me$_3$Bzm, which have ϕ angles with absolute values between 0° and 23°,[5] exhibit almost exclusively the A-type structure. Of the four *N*-MeImd structures reported here, the R = CH$_2$CN and Cl complexes exhibit the normal A-type orientation, as does the reported R = adam structure.[28] Complexes with R = CH$_2$CH$_3$ and CH$_3$ have B-type structures, along with the structure reported for *N*-MeImdCo(DH)$_2$CH$_2$CH$_2$CN.[29]

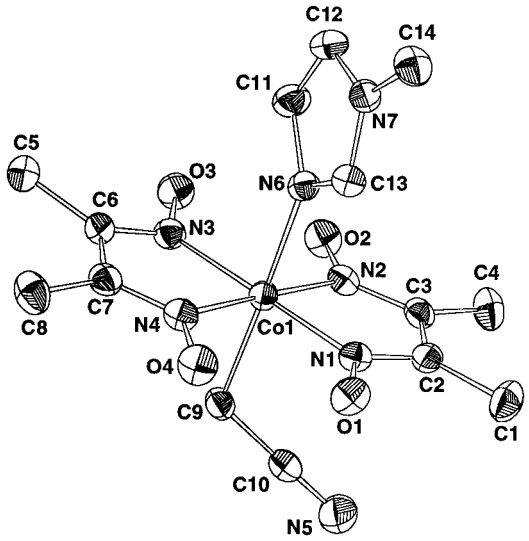

Figure 3. ORTEP drawing of *N*-MeImdCo(DH)$_2$CH$_2$CN (**3**). Ellipsoids are shown at the 50% level. H atoms are omitted for clarity.

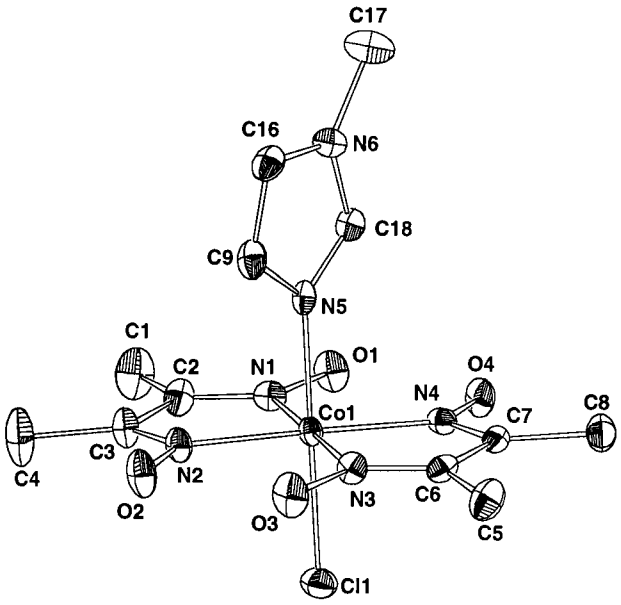

Figure 4. ORTEP drawing of *N*-MeImdCo(DH)$_2$Cl (**4**). Ellipsoids are shown at the 50% level. H atoms are omitted for clarity.

(b) Axial Fragment and *N*-MeImd Coordination. A comparison of the geometry around the coordinated axial N for the *N*-MeImd complexes appears in Table 2. The Co−N$_L$ bond lengths increase with increasing electron-donating ability of the trans ligand, as expected from analogous series of py and Me$_3$Bzm cobaloximes.[5,8] For the *N*-MeImd cobaloximes, the Co−N$_L$−I2 and Co−N$_L$−I4 angles average 126.5° and 127.9°, respectively. In the Me$_3$Bzm complexes, the averages of the comparable Co−N$_L$−B2 and Co−N$_L$−B9 angles are 121.6° and 133.4°, respectively,[5] reflecting the need to accommodate the lopsided bulk of Me$_3$Bzm in these complexes.

(28) Bresciani-Pahor, N.; Randaccio, L.; Zangrando, E.; Summers, M. F.; Ramsden, J. H., Jr.; Marzilli, P. A.; Marzilli, L. G. *Organometallics* **1985**, *4*, 2086.
(29) Bresciani-Pahor, N.; Attia, W. M.; Geremia, S.; Randaccio, L. *Acta Crystallogr., Sect. C* **1989**, *45*, 561.

Table 2. Structural Comparison of $LCo(DH)_2R$ Complexes

	Co−N_L (Å)	Co−C (Å)	Co−N−I2 (deg)	Co−N−I4 (deg)	α (deg)	ϕ (deg)
			L = *N*-MeImd			
adamantyl[a]	2.065(4)	2.154(5)	127.4(3)	127.8(3)	−10.0	∼0
CH_2CH_3	2.047(3)	2.023(4)	126.6(2)	128.1(2)	2.1	−60.5
CH_2CH_2CN[b]	2.037(3)	1.989(5)	125.4(2)	129.0(2)	4.9	−67.0
CH_3	2.032(3)	1.980(4)	126.7(2)	127.9(2)	4.1	−66.2
CH_2CN	1.989(2)	2.010(2)	126.5(1)	127.3(2)	−3.7	22.5
Cl	1.936(3)		126.3(2)	127.2(2)	1.3	−9.17
			L = Me_3Bzm			
adamantyl[c]	2.137(4)	2.179(5)	120.8(4)	134.4(3)	−6.1	22.6
CH_2OCH_3[d]	2.093(2)	2.033(3)	122.0(2)	132.9(2)	2.8	−3.6
$CH(CH_3)_2$[e]	2.097(2)	2.076(2)	120.9(2)	134.4(1)	4.0	6.6
CH_2CH_3 [f]	2.084(5)	2.027(5)	122.6(3)	132.8(3)	4.0	∼0
CH_3[e]	2.060(2)	1.989(2)	121.5(2)	133.6(1)	4.7	13.9
$CHCl_2$[g]	2.043(2)	1.983(2)	121.6(1)	133.2(1)	1.5	−10.3
CH_2NO_2[e]	2.013(3)	1.988(5)	122.4(3)	132.7(3)	4.8	−18.7
CH(CN)CHCN[h]	2.031(3)	2.061(3)	121.1(3)	133.7(3)	3.1	3.7
Cl[e]	1.959(3)		121.1(2)	133.6(2)	1.1	−0.7

[a] Reference 28. [b] Reference 29. [c] Reference 31. [d] Reference 21. [e] Reference 5. [f] Reference 32. [g] Reference 33. [h] Reference 34.

Chart 2

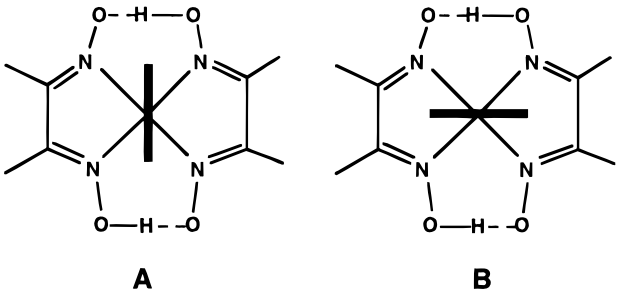

Table 3. $^1J_{CH}$ (Hz) Data for $Me_3BzmCo(DH)_2R$ Complexes in $CDCl_3$

R/X	$^1J_{BH2}$	$^1J_{BH4}$	$^1J_{BH7}$	$^1J_{BH10}$	$^1J_{BH11}$	$^1J_{BH12}$
free[a]	203.7	158.8	157.5	126.2	126.1	139.4
adamantyl[a]	207.2	163.6	158.5	125.9	125.8	139.8
CH_2OCH_3[b]	207.8	163.5	159.0	126.1	125.8	140.1
$CH(CH_3)_2$[b]	207.9	163.3	159.0	126.1	125.7	140.1
CH_2CH_3[a]	208.0	163.3	159.0	126.3	126.1	140.3
CH_3[a]	208.2	163.3	159.2	126.2	126.0	140.4
CH_2Br	208.7	163.6	159.6	126.5	126.5	140.6
CH_2CF_3	208.6	164.1	159.4	125.9	126.0	140.6
$CHCl_2$	208.9	164.2	160.0	127.1	126.6	140.5
CH_2CN	208.6	163.7	159.8	126.7	126.5	140.7
CH_2NO_2[a]	209.1	163.7	159.8	126.7	126.5	140.9
$CH(CN)CH_2CN$	208.6	164.1	159.8	126.4	126.4	140.8
N_3	209.6	165.0	160.6	126.6	126.6	141.3
Cl[a]	209.9	164.8	160.4	126.6	126.5	141.2
free H^+ [a]	218.6	166.5	163.2	overlap	overlap	143.4

[a] Reference 4. [b] Reference 21.

Coupling Constants. The $^1J_{CH}$ values for all of the Me_3Bzm and *N*-MeImd complexes are reported in Tables 3 and 4, respectively. Coupling constants for L generally increase from free ligand values as the electron-donating ability of the trans ligand decreases. For the Me_3Bzm complexes, these values do not exceed those of the protonated ligand. Data on a soluble protonated *N*-MeImd salt could not be obtained for comparison. The carbon in the 2 position (between the two N's) of both L's shows the largest range of coupling constants (Table 4). This same carbon shows almost no change in the ^{13}C shift over the series of R's (Figures 5 and 6).

Correlations between $^1J_{CH}$ and ^{13}C NMR Shifts. Plots of the L group $^1J_{CH}$ values against the ^{13}C chemical shifts for both the Me_3Bzm and *N*-MeImd complexes generated a wide range of r_a^2 values (Supporting Information). The analysis revealed good correlations ($r_a^2 \geq 0.90$) between the B5 ^{13}C shift and 1JBH2, $^1J_{BH7}$, $^1J_{BH12}$; the B6 shift and $^1J_{BH7}$, $^1J_{BH12}$; the B7 shift and $^1J_{BH12}$; the B4 shift and $^1J_{BH12}$; and the B10 shift and $^1J_{BH7}$, $^1J_{BH12}$. In the *N*-MeImd series of complexes, good correlations ($r_a^2 \geq 0.90$) were identified between the I5 ^{13}C shift and $^1J_{IH1}$; and between the I1 shift and $^1J_{IH1}$, $^1J_{IH5}$. In the Me_3Bzm series, $^1J_{BH4}$, $^1J_{BH10}$, and $^1J_{BH11}$ exhibited very poor correlations with the ^{13}C chemical shift for all positions. Similarly, the Me_3Bzm B2, B8, B9, B11, and B12 ^{13}C shifts produced low r_a^2 values when plotted against all $^1J_{BH}$ values.

Table 4. $^1J_{CH}$ (Hz) Data for *N*-MeImdCo$(DH)_2$R Complexes in $CDCl_3$

R/X	$^1J_{IH1}$	$^1J_{IH2}$	$^1J_{IH4}$	$^1J_{IH5}$
free	139.4	205.7	189.6	188.1
adamantyl	140.3	210.2	194.3	191.5
CH_2OCH_3	140.5	210.0	193.8	191.4
$CH(CH_3)_2$	140.5	209.8	193.7	191.1
CH_2CH_3	140.5	210.2	194.1	191.6
CH_3	140.6	210.4	194.2	191.8
CH_2Br	140.8	211.0	194.7	192.3
CH_2CN	141.0	210.9	195.4	193.2
$CH(CN)CH_2CN$	141.2	211.1	195.4	193.6
Cl	141.6	212.3	196.6	195.0

Inter-Series Correlations. The ^{13}C shifts were compared between the *N*-MeImd and Me_3Bzm series (Supporting Information). The B4, B6, B7, and B10 shifts correlated strongly with both the I1 and I5 shifts ($r_a^2 \geq 0.90$). Good correlations were also observed for B9 and B12 shifts with I1 and for B5 shifts with I5. No significant correlations were found involving I2, I4, B2, B8, and B11 shifts. Similarly, the $^1J_{CH}$ values were compared between the two series of complexes (Supporting Information). The only significant correlations ($r_a^2 \geq 0.90$) between the two series were $^1J_{IH1}$ with $^1J_{BH7}$ and $^1J_{BH12}$.

Correlations with Alkyl Ligand Parameters. All ^{13}C shifts and $^1J_{CH}$ values were plotted against three parameters used to describe the electron-donating ability of the R group in cobaloximes, namely, Co−N_L bond distance[5,21] (Table 2), EP,[8] and Randaccio and co-workers' t_1 scores[13] (Supporting Information). The r_a^2 values for these single parameter fits are presented in Table 5. The B2 and I2 ^{13}C shifts were poorly fit with each of the three parameters (e.g., EP in Figures 5 and 6), as were the I4 shifts. For the C's bound to the coordinating N, only the B9 shifts correlated moderately well. In fact, B9 shifts correlated strongly with EP ($r_a^2 = 0.9623$, Figure 7). The Me_3Bzm B5, B6, and B10 shifts displayed strong correlations

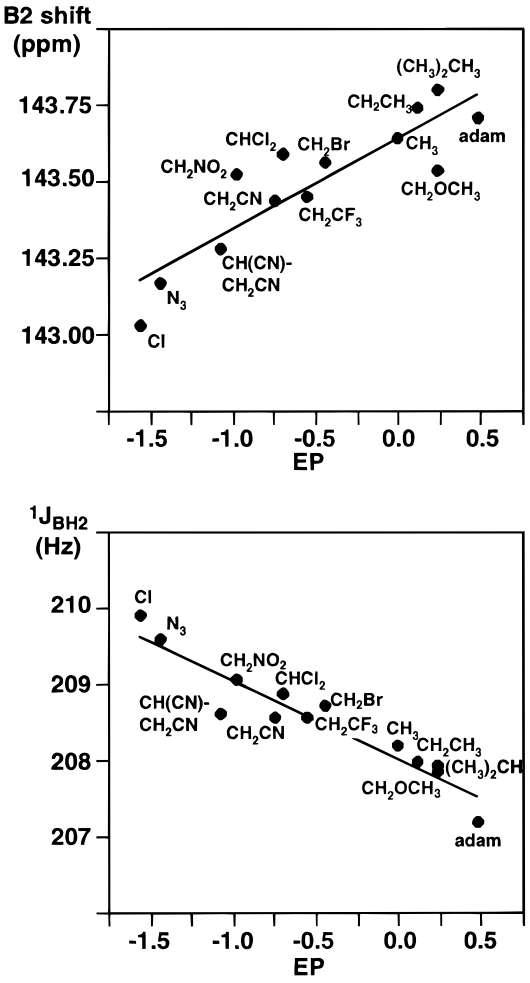

Figure 5. Plots of ^{13}C and $^{1}J_{CH}$ values vs EP for the 2 position of Me_3Bzm complexes.

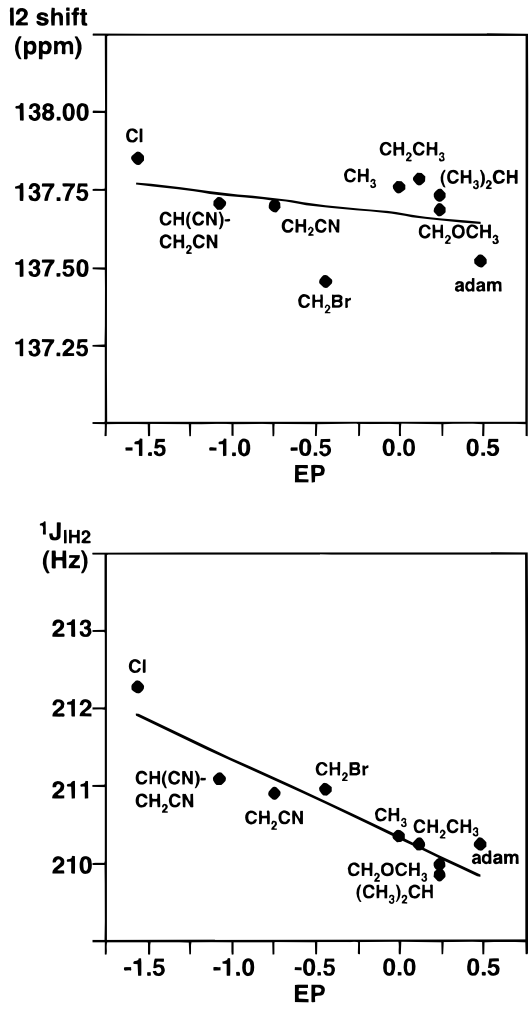

Figure 6. Plots of ^{13}C and $^{1}J_{CH}$ values vs EP for the 2 position of *N*-MeImd complexes.

with all three electronic terms, while the B4, B7, and B12 shifts correlated strongly with EP only. The remoteness of B11 from the Co resulted in small changes in ^{13}C shift and $^{1}J_{CH}$ values, leading to insignificant correlations (Table 5). In the *N*-MeImd complexes, I5 and I1 produced the only significant correlations between the ^{13}C shift and the ligand parameters (Co−N_L and EP). In fitting the $^{1}J_{CH}$ values as a function of trans ligand electron donation, the strongest correlations were observed with Co−N_L and EP for $^{1}J_{BH2}$, $^{1}J_{BH7}$, and $^{1}J_{BH12}$ in the Me_3Bzm complexes and $^{1}J_{IH4}$, $^{1}J_{IH5}$, $^{1}J_{IH6}$ in the *N*-MeImd complexes.

Randaccio and co-workers' multiparameter description of various solid state and solution properties produced a new parameter set composed of three *t* scores[13] as described below. Application of this three-parameter set to our ^{13}C shift and coupling data produced equations of the type $Y = a_1t_1 + a_2t_2 + a_3t_3 + c$ (where $Y = {}^{13}C$ shifts or $^{1}J_{CH}$ values). The ANOVA tables generated during the data fitting procedures provided values (*p*) for the significance of each *t* score in the data fit (Supporting Information). Because of the larger data set, the Me_3Bzm values produced better results.

Table 5. Coefficients of Determination (r_a^2) for Fitting ^{13}C Shifts and $^{1}J_{CH}$ Values with Trans Influence Parameters

	^{13}C shifts			$^{1}J_{CH}$		
	Co−N	EP	t_1	Co−N	EP	t_1
	($n = 9$)	($n = 13$)	($n = 10$)	($n = 9$)	($n = 13$)	($n = 10$)
B2	0.6560	0.7653	0.4710	0.9676	0.8879	0.9028
B4	0.8629	0.9742	0.8506	0.5532	0.6713	0.2631
B5	0.9471	0.9451	0.9380			
B6	0.9297	0.9899	0.9121			
B7	0.8752	0.9659	0.8471	0.9168	0.9199	0.8987
B8	0.6999	0.8205	0.5211			
B9	0.8794	0.9623	0.7936			
B10	0.9158	0.9369	0.9519	0.3728	0.3038	0.3235
B11	0.0700	0.1543	0.0000	0.6187	0.6693	0.6472
B12	0.8674	0.9776	0.8004	0.9710	0.9320	0.9456
	($n = 5$)	($n = 9$)	($n = 7$)	($n = 5$)	($n = 9$)	($n = 7$)
I1	0.9777	0.9822	0.7657	0.9899	0.9820	0.8429
I2	0.2532	0.0000	0.0847	0.8934	0.8631	0.6099
I4	0.0000	0.0000	0.0000	0.9192	0.8958	0.5803
I5	0.9650	0.9677	0.8380	0.9520	0.9421	0.6795

Discussion

X-ray Structures. Planar axial ligands have been found to adopt the A-type orientation (Chart 2) in cobaloximes, the only reported exceptions being *N*-MeImd complexes. In three previously reported structures (R = CH_3, OH, and CH_2CH_2CN),[28,29] *N*-MeImd adopts the unusual B-type orientation (Chart 2). We found that *N*-MeImd in crystals of complexes with R = CH_2CH_3 (**1**) and CH_3 (**2**) also has the B-orientation. In **1**, **2**, and the complex with R = CH_2CH_2CN, butterfly bending is away from the L group (positive α values). In contrast, the A-type L orientation was found here when R = CH_2CN (**3**). Butterfly bending of the equatorial plane toward the *N*-MeImd (negative α values) for **3** and for the adamantyl complex creates a groove that bisects the O−H- - -O bridges and forces the *N*-MeImd into the A-orientation. Since the CH_2CN ligand is

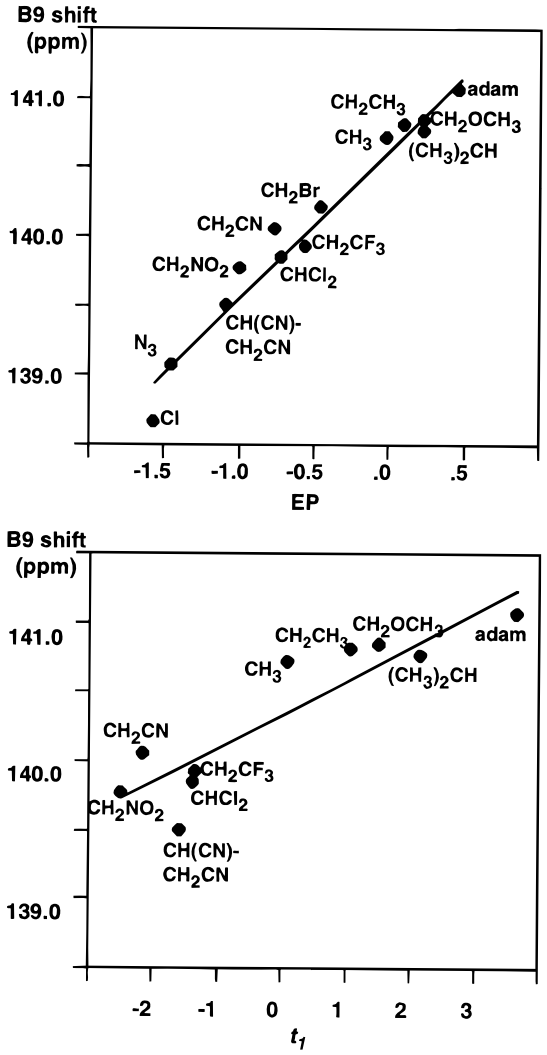

Figure 7. Plots of B9 shift vs EP and t_1.

not sterically demanding, the butterfly bending toward *N*-MeImd probably arises from crystal packing effects. The chloro complex (**4**) also has butterfly bending away from *N*-MeImd, but this bending is small. Our findings suggest that a steric threshold exists close to a relatively planar $Co(DH)_2$ equatorial moiety (α values $\sim$ 0°); the B orientation of *N*-MeImd is sterically allowed only when butterfly bending is away from *N*-MeImd (i.e., $\alpha > 0$).

In no case does Me_3Bzm adopt the B-orientation. The difference in the steric requirements of Me_3Bzm and *N*-MeImd is evident on inspection of the Co−N_L−C angles of the complexes. For the lopsided Me_3Bzm, these angles average ∼122° and ∼133° for Co−N_L−B2 and Co−N_L−B9, respectively,[5] whereas the analogous angles in *N*-MeImd complexes average ∼127° and ∼128°, respectively. The nearly equal values for the *N*-MeImd angles indicate smaller steric requirements than those imposed by the benzene ring on the Me_3Bzm. We believe this comparison indicates that differences in molecular orbitals of these L cannot be responsible for the differences in L orientation. Furthermore, there is no relationship between the electronic properties of the trans ligand and the orientation of *N*-MeImd. *N*-MeImd is simply a much smaller ligand than the lopsided Me_3Bzm. Therefore, when butterfly bending is away from *N*-MeImd, the *N*-MeImd can adopt the A- or the B-orientation.

Measures of the Trans Influence. Throughout our study, the influence of the trans axial ligand on the $^1J_{CH}$ and ^{13}C NMR shifts for the Me_3Bzm and *N*-MeImd cobaloxime series was assessed using three measures of the trans influence: Co−N_L bond distances, EP values, and *t* scores. The first two of these measures are determined more or less directly from experimental quantities. As such they reflect the net of both steric and electronic effects. The Co−N_L distances are an excellent measure of the trans influence but are not so easily obtained as spectroscopic data. Therefore, any analysis is limited by the amount of X-ray data available. The EP values, which are based on ^{13}C shifts of py cobaloximes, encompass a large range of ligands and have shown excellent correlations with Co−N_L distances. Furthermore, this parameter has been applied successfully to cobaloximes with diverse L as well as to other B_{12} model systems.[3,5,19,30]

Randaccio and co-workers analyzed both Co−N_L distances and the ^{13}C shifts for pyridine cobaloximes with the *t* scores resulting from their use of principal component analysis (PCA).[13] The PCA method generated three *t* scores for each R, one representing the electronic (inductive and resonance) properties of R (t_1), one representing the steric bulk of R (t_2), and one believed to reflect a contribution from the Co−Ca−Y angle (t_3). These three scores represent the mathematical separation of the influences contributing to experimentally observed structural (Co−C, Co−N_L, and *d*), spectroscopic (γ-^{13}C shifts), and kinetic (log *k* for py dissociation) data.[13] Their analysis indicated that (i) the Co−N_{py} distance is predominantly influenced by t_1, with a small contribution from t_3; and (ii) the ^{13}C shifts of the remote γ-C of py used in determining EP are affected predominantly by t_1 but also by t_2.[13] Thus, neither the Co−N_{py} distances nor the py γ-^{13}C shifts reflect the electronic trans influence of R without other contributing factors. However, the major limiting factor in extending the PCA approach to other R ligands is the extensive database necessary for determining the *t* scores. Our use of the three *t* scores was restricted primarily to the Me_3Bzm data because of the lack of *t* scores for Cl. The weak-donor R groups are underrepresented in our *N*-MeImd series with respect to the Me_3Bzm series.

NMR Spectroscopy. Both ^{13}C shifts and $^1J_{CH}$ values exhibited trends over the two series of complexes investigated. Interpretable trends in ^{13}C shifts were possible only for carbons in positions remote from the Co. In general, the ^{13}C shifts correlated more strongly with EP than with Co−N_L bond distances. The B5, B6, and B10 shifts show strong correlations with all three inductive parameters in the simple linear fits (Table 5). Furthermore, the significance of t_1 clearly dominates in the multiparameter analysis of these shifts (Supporting Information). The positions of B5, B6, and B10 are remote enough from the Co binding site to minimize the through-space effects of the metal but close enough to show an appreciable and predictable change in response to the variation of R. The $^1J_{CH}$ values for both series of complexes increased as the electron-donating ability of R decreased (Tables 3 and 4), as we previously observed for a smaller sample of Me_3Bzm complexes.[4]

In both Me_3Bzm and *N*-MeImd complexes, the 2 position displayed the largest range of $^1J_{CH}$ values over the R series.

(30) Bresciani-Pahor, N.; Geremia, S.; Lopez, C.; Randaccio, L.; Zangrando, E. *Inorg. Chem.* **1990**, *29*, 1043.
(31) Bresciani-Pahor, N.; Attia, W. M.; Randaccio, L.; Lopez, C.; Charland, J.-P. *Acta Crystallogr., Sect. C* **1987**, *43*, 1484.
(32) Solans, X.; Gómez, M.; López, C. *Transition Met. Chem.* **1991**, *16*, 176.
(33) Chen, Q.; Marzilli, L. G.; Bresciani-Pahor, N.; Randaccio, L.; Zangrando, E. *Inorg. Chim. Acta* **1988**, *144*, 241.
(34) Charland, J.-P.; Attia, W. M.; Randaccio, L.; Marzilli, L. G. *Organometallics* **1990**, *9*, 1367.

However, the ^{13}C shifts showed relatively little change. Furthermore, the ^{13}C shifts for this carbon showed little or no dependence on variation in R in either series (Figures 5 and 6). In fact, when B2 and I2 shifts are each plotted against EP (Figures 5 and 6), the least-squares fits produce equations with slopes of opposite sign. In Me_3Bzm cobaloximes, except for B2 and B8, we found strong correlations with the EP values for all the available ^{13}C data (Table 5). The failure of the *t* scores in the multiparameter fit to contribute significantly to a description of the change in B2 shift as a function of R suggests that an anomalous effect that was not included in the PCA approach must be contributing to B2 shifts, since electronic and steric parameters appear unable to describe the observed shifts.

The good correlations observed for $^1J_{BH2}$, $^1J_{BH7}$, $^1J_{BH12}$, $^1J_{IH4}$, $^1J_{IH5}$, and $^1J_{IH6}$ with both Co−N_L bond distance and EP (Table 5) indicate that the coupling constants reflect in a highly satisfying manner the changes within the ligand. The multiparameter *t* score analysis of $^1J_{BH2}$, $^1J_{BH7}$, and $^1J_{BH12}$ values shows very high significance for the t_1 term and no significant contribution from t_2 and t_3 (Supporting Information), suggesting that the coupling constants for these three positions of the Me_3Bzm ligand provide an excellent probe of the electronic trans influence of R on this ligand. Clearly, the coupling constants reflect a predictable response to the electron donation of R not observed with close-in ^{13}C shifts.

Furthermore, the coupling constants can be expressed as the percentage of s character (ρ) contributed to the CH bond by the C atom according to $^1J_{CH}$ (Hz) = 500 ρ_{CH}.[10,11] For comparison, values of 125, 166.67, and 250 Hz represent pure sp^3, sp^2, and sp systems, respectively. In unbound Me_3Bzm and *N*-MeImd, the C orbitals contributing to the CH bond for the position between the N's have 40.86 and 41.14% s character, respectively. The coupling constant for the protonated Me_3Bzm corresponds to 43.72% s character for the same position. When coordinated to Co in cobaloximes, the percentage s character for the 2 position increases to a range of 41.44−41.98% and 42.05−42.46% for Me_3Bzm and *N*-MeImd, respectively, following the trend of decreasing electron-donating ability. These results are consistent with increasing p character in the CN bonds, leading to increasing s character in the CH bond.

The smaller range of $^1J_{CH}$ values for I2 vs B2 in response to the changing trans influence may be a result of the differing orientations of *N*-MeImd. The $^1J_{IH}$ values for *N*-MeImd in the R = adam complex are greater than expected from the trend of electron-donating ability. The rotation of L ligands means that the $^1J_{CH}$ values reflect the weighted average of all species. In more sterically hindered complexes such as R = adam, the observed $^1J_{CH}$ value would reflect the preference of the A-orientation, whereas the B-orientations may be relatively more favored for complexes with other trans axial ligands. This effect appears to be small, however.

Steric Influences on the Benzene Ring. The size of the Me_3Bzm moiety favors the A-orientation, but steric interactions between the benzene ring and the equatorial ligand plane still exist and account for the structural features of the Me_3Bzm complexes.[5,19] Trends in NMR shift data have also suggested that steric effects are important for Me_3Bzm.[5,19] The relatively poor correlation of $^1J_{BH4}$ values with the trans influence parameters is noteworthy since $^1J_{BH7}$ and $^1J_{BH12}$ involving carbons more distant from the coordinating N have values that correlate well with such parameters. Steric effects, e.g., compression of the BH4 bond as a result of nonbonded interactions with the equatorial $(DH)_2$ moiety, may be responsible. Indeed, the results of the application of the *t* scores to $^1J_{BH4}$ values indicate similar significance levels for the t_1 and t_2 terms, which reflects the steric bulk of R (Supporting Information).

The poor correlations between B8 shifts and Co−N_L distances and t_1 scores but a moderate fit for the same shift data with EP (Table 5) also appear to be due to a steric interaction. The better correlation between B8 and EP may once again reflect the contribution of a steric effect in the value of EP. In addition, in the multiparameter fit of Me_3Bzm shifts with the *t* scores, B8 has a greater significance (lower *p* value) for the steric term (t_2) compared to the significance of t_2 for other Me_3Bzm shifts as a function of R, including B9. The latter correlates well with EP (Figure 7). Thus, the B8 shifts appear to reflect the steric effect more than the shifts of other Me_3Bzm carbons. The poor correlation between B8 shifts and the shifts of the analogous I5 carbon of the smaller *N*-MeImd ligand further suggests a steric influence.

Conclusions

Changes in the properties of imidazole-type ligands are reflected in the magnitude of the $^1J_{CH}$ values of the imidazole ring in a relationship which is unaffected by anisotropic effects and minimally affected by steric effects. In contrast, especially for bulky ligands, the shifts of close-in carbons and even remote carbons of such ligands appear to be influenced by steric effects. The recently introduced *t* scores from the PCA investigation of Randaccio and co-workers are a valuable new set of parameters for interpreting such spectroscopic data. The structural results support the view that imidazole is a relatively small planar ligand; thus, its orientation is less subject to steric effects caused by nonbonded interactions with the equatorial ligand than other ligands such as benzimidazoles and pyridines. When the trans ligand is not bulky, imidazole ligands frequently appear to adopt the B-orientation, at least in the solid state.

Acknowledgment. This work was supported by NIH Grants GM 29225 and GM 29222 (to L.G.M.). The authors also wish to thank Suzette Polson, Hao Ni, Jennifer J. Cowan, and Alexander Kutikov for preparing some of the complexes, and Dr. Karl Hagen and Scott L. Childs for their assistance with the *N*-MeImdCo$(DH)_2$Cl structure.

Supporting Information Available: Tables of elemental analyses, complete bond lengths and angles, hydrogen atom coordinates, anisotropic thermal parameters;, NMR data including ^1H and ^{13}C NMR shifts and equatorial ligand $^1J_{CH}$ values, statistical results, structural comparison between **2** and the previously published X-ray structure, and parameters for the assessment of ligand trans influence (27 pages). Ordering information is given on any current masthead page.

IC980519K